

Discovery of a Near-Infrared Jet-Like Feature in the Z Canis Majoris System

R. Millan-Gabet¹ and J. D. Monnier²

Harvard-Smithsonian Center for Astrophysics, Cambridge, MA 02138

rmillan@cfa.harvard.edu, jmonnier@cfa.harvard.edu

ABSTRACT

We present near-infrared high resolution observations of the young binary system Z Canis Majoris using the adaptive optics system at the Keck-II telescope. Both components are unresolved at 1.25 μm and 1.65 μm , although high dynamic range images reveal a previously unknown jet-like feature in the circumstellar environment. We argue that this feature probably arises from light scattered off the walls of a jet-blown cavity, and proper motion studies of this feature can probe the dynamics of the bipolar outflow. Potentially, the morphology of the dust-laden cavity walls offers a new probe of the momentum profile and collimation of bipolar winds from young stellar objects. We also derive high precision binary parameters, which when combined with historical data have allowed the first detection of orbital motion. Lastly, our observations confirm the high degree of flux variability in the system; the North-West binary component is dominant at H-band, in contrast to all previous observations.

Subject headings: instrumentation: adaptive optics—techniques: high angular resolution—stars: formation—planetary systems: protoplanetary disks—infrared: stars

1. Introduction

Z Canis Majoris (Z CMA) is a luminous and irregularly variable young stellar object (YSO) originally classified as a Herbig Ae/Be star (HAeBe, intermediate to high mass pre-main sequence stars) on the basis of its emission line spectrum and association with reflection nebulosity (Herbig 1960). It underwent an outburst lasting a few months in 1987, during which its spectral characteristics drastically changed and its visual brightness increased by a modest ~ 0.7 magnitudes (Hessman et al. 1991). High resolution optical and near-infrared (IR) spectra in the post-outburst state showed features typical of the FU Orionis (FUOri) class, believed to be disk objects undergoing a period of very active accretion (Hartmann et al. 1989). Under this interpretation, Z CMA is unique in that it is the YSO with the highest known accretion rate ($\sim 10^{-3}M_{\odot} \cdot \text{yr}^{-1}$). The ranges of visual and near-IR magnitudes of the unresolved system found in the literature are: V=11.20 – 8.80, J=6.16 – 5.87, H=5.09 – 4.70 and K=3.4 – 4.2.

A companion was discovered in IR speckle observations by Koresko et al. (1991). The binary system had an angular separation of 0.1'' and position angle PA=120° (measured East from North), where the primary

¹now at: Caltech, Interferometry Science Center, Pasadena, CA 91125

²now at: University of Michigan, Ann Arbor, MI 48109

is defined to be the North-West (NW) component, which dominates the flux beyond $2.2\ \mu\text{m}$. Individual spectral energy distributions reconstructed from the spatially resolved photometry, combined with unresolved photometry at optical and far-IR wavelengths, revealed that the emission in both components is dominated by circumstellar material, i.e. there are no signs of stellar photospheres. The South-East (SE) component has been identified as the FU Ori object inferred by Hartmann et al. (1989), while the NW component is most-likely a HAeBe star surrounded by an asymmetric dust envelope (e.g., Garcia, Thiébaud, & Bacon 1999).

In the last few years, HAeBe and FU Ori objects have also been resolved using the techniques of long baseline interferometry and aperture masking at near-IR wavelengths (Malbet et al. 1998; Akeson et al. 2000; Millan-Gabet, Schloerb, & Traub 2001; Tuthill, Monnier, & Danchi 2001; Danchi, Tuthill, & Monnier 2001). However, the interpretation of the interferometer data depends on important model assumptions, namely the extent to which the measured visibilities are systematically reduced (which results in an overestimate of the size measured) by flux arising in a widely-separated companion or scattered by distant dust.

The discovery reported here took place in the larger context of a program of adaptive optics (AO) observations of HAeBe systems, aimed at providing these constraints by exploring the level of extended emission present at spatial scales intermediate between the very narrow interferometric beams and the large scale nebulosity known to surround these systems.

2. Observations

We observed Z CMa on 2001 January 11, using the AO system at the Keck-II telescope (Wizinowich et al. 2000). These observations were carried out using the slit viewing camera (SCAM) of the NIRSPEC instrument (McLean et al. 2000) as the imaging science detector. In these observations, Z CMa itself – unresolved by the Shack-Hartmann sensor sub-apertures – was used as the source of visible photons for the AO wavefront sensor. In order to achieve highest sensitivity to scattered emission from circumstellar material, we limited our observations to the shorter wavelength near-IR bands: J (N3 filter, $\lambda = 1.143 - 1.375\ \mu\text{m}$) and H (N5 filter, $\lambda = 1.413 - 1.808\ \mu\text{m}$).

Our observing procedure consisted of establishing the maximum integration time per frame which did not saturate the bright stellar core, and co-adding 30 such frames. For all frames the correlated double sampling (CDS) readout mode was used. In order to search for circumstellar emission beyond the normal field of view of the SCAM array in AO mode ($4.3 \times 4.3''$) and to improve the image quality – by removing the effect of the NIRSPEC slit – we recorded 4 such frames nodding the telescope around a square by offsets of $4.3''/2$, which resulted in a total field of view in the combined image of $6.45 \times 6.45''$. We also recorded J-band frames in which the central core was allowed to saturate the detector, in order to further augment our sensitivity to faint extended emission.

The results presented here have been obtained from the AO-corrected images, after straightforward processing (i.e. no deconvolution has been applied) consisting of: bad pixel removal, flat field correction (using images of near-sunrise sky) and sky background subtraction (using images obtained with a telescope offset of $60''$ from the target source).

As an indication of the seeing quality and performance of the AO system at the time of our Z CMa observations, the images of an unresolved calibrator star – HD 54335, chosen to also have similar visual and near-IR magnitude as Z CMa – were fitted with the sum of two Gaussians of different widths, representing the

narrow core and wide halo into which partially corrected point spread functions (PSF) can be approximately decomposed. Using the full-width at half-maximum of the core component as a measure of effective seeing, we find on average 45 mas and 46 mas at J and H bands respectively, both close to the diffraction limit of the 10 m telescope (31 and 42 mas respectively). For this analysis, as well as in the rest of the paper, stellar images are fitted with sub-pixel resolution using 2-dimensional pixelized Gaussians.

3. The Z CMa Binary

We first derive the basic parameters of the Z CMa binary from our images. A model consisting of two scaled and displaced Gaussians gives us the binary separation, PA, and flux ratio. These parameters are derived for each of the N frames in our dithering procedure, and the final value adopted is the mean of these independent measurements, with a statistical error given by their standard deviation.

The plate scale and orientation of the AO images were calibrated using observations of the quadruple system ξ Ursae Majoris (HD 98230) and its published orbital elements (Mason, McAlister, Hartkopf, & Shara 1995). Given that the published orbit applies to the “Aa” center of mass and “B” component (the “a” component was unresolved until recent, unpublished, Keck Aperture Masking observations in June 2000 by one of the authors – J. D. Monnier), we estimated the location of the former in our images using the published masses (Heintz 1967). Assigning 10% and 30% mass uncertainties to the “A” and “a” components respectively, we obtain a plate scale of 17.32 ± 0.06 mas/pixel (1.9% different than nominal value of 17 mas/pixel) and a PA offset (calculated – nominal) of $-1.18 \pm 0.18^\circ$.

These results are summarized in Table 1. In addition, our $1.25 \mu\text{m}$ and $1.65 \mu\text{m}$ measurements are consistent with both binary components being unresolved; that is, we find no evidence for the extended component reported by Malbet et al. (1993) at somewhat longer wavelengths ($\lambda > 3.87 \mu\text{m}$).

Figure 1 shows the history of measurements of the Z CMa orbital elements up to this work (Koresko et al. 1991; Haas et al. 1993; Barth, Weigelt, & Zinnecker 1994; Thiebaut et al. 1995) spanning a total of 11.2 years, and linear fits to the data. While only a marginal change in the angular separation is detected ($\chi^2_{reduced} = 0.3$ for the linear fit, compared to 0.8 for the weighted mean), the PA has clearly increased over this period of time ($\chi^2_{reduced} = 0.6$ for the linear fit, compared to 5.8 for the weighted mean), making this the first detection of orbital motion in this system.

The linear fit to the PA data gives a total change of $8.8 \pm 1.5^\circ$. For a distance to Z CMa of about 1150 pc (Herbst, Racine, & Warner 1978), the $\sim 0.1''$ angular separation corresponds to a projected linear separation of 115 AU. Assuming masses for the components of $1M_\odot$ and $5M_\odot$, typical of T Tauri and HAeBe stars respectively, the period of a face-on circular orbit would be ~ 500 years, and the expected rate of position angle change ~ 0.7 degrees/year. Therefore, our detection of a 8.8° change in about a decade is indeed plausible.

Previous workers have found the near-IR flux ratios to be highly variable: $[NW/SE]_J = 0.09 - 0.3$, $[NW/SE]_H = 0.25 - 0.5$ and $[NW/SE]_K = 1.6 - 3.3$ (Koresko et al. 1991; Haas et al. 1993). As can be seen in Table 1, we find the unexpected result that the NW (HAeBE) component becomes brighter than the SE (FU Ori) component at H-band, in contrast to previous reports that the NW component became the brightest in the system at K-band and longer wavelengths. This flux reversal could be naturally explained if the FU Ori object has been continuously fading following its recent outburst. Approximate absolute photometry may be derived from our observations as follows.

The total flux of the Z CMa system at our epoch is estimated using the calibrator (HD 54335) as a flux standard. Its 2MASS fluxes are: $F_J(\text{HD 54335}) = 19 \pm 4$ Jy and $F_H(\text{HD 54335}) = 31 \pm 6$ Jy. From our images we derive a ratio of fluxes between Z CMa and HD 54335 of 1.39 ± 0.08 and 2.68 ± 0.25 at J and H bands respectively. The resulting combined fluxes of Z CMa as well as those of its components, derived using our estimates of the sum and ratio of fluxes, are also given in Table 1. Indeed, these estimates clearly show that the FU Ori object has been dimming between 1986 and 2001. In particular, comparing with the epoch of the Koresko et al. (1991) observations, the SE fluxes have decreased by $\sim 1.1 \pm 0.4$ mag and $\sim 0.7 \pm 0.3$ mag at J and H bands respectively. In contrast, the HAeBe photometry is consistent with no flux change at J band ($\Delta m_J \simeq 0.1 \pm 0.5$) and a marginally significant increase at H band ($\Delta m_H \simeq 0.5 \pm 0.4$).

4. High Dynamic Range Imaging: Discovery of a New Jet-Like Feature

4.1. Image Processing

We have detected a new jet-like feature in deep images at J-band in which the stellar cores were saturated. Unfortunately, there are many imaging artifacts in such high-dynamic range images, and we will briefly mention the dominant ones before discussing the “jet-like” feature discovered around Z CMa. In Figure 2 we show the mosaiced images of Z CMa and the unresolved reference star (HD 54335), in which an azimuthally-averaged PSF core has been subtracted to artificially enhance the dynamic range in the image. We have marked the dominant artifacts common to the both Z CMa and the reference star, but note the interesting new feature *not* associated with the PSF. Prior to this detection, no extended structure was known for Z CMa at these wavelengths and scales (< 1 arcsec) beyond that of a pure binary (nebulousity on larger scales has been reported by Nakajima & Golimowski 1995).

Figure 3 shows a close-up of the region near the new narrow feature, rotated so that North is up and East is left. In order to remove the wings of the PSF, we have subtracted a two-component model of the binary star using the PSF measured with the reference star. Clearly this subtraction is imperfect, as evidenced by the speckled residuals within $0.5''$ of the binary. Despite these obvious flaws, the dynamic range (DR) in the image (unsaturated peak to noise ratio) is ~ 200000 beyond $\sim 0.5''$ from the central binary, and the signal-to-noise in the jet-like feature is greater than 10. The jet-like feature extends to $\sim 0.9''$ (1135 AU) from the central binary in the S-SW direction, and has a width of $\sim 0.1''$ (115 AU).

4.2. Discussion

It is likely that the extended emission we have detected is stellar light or disk emission scattered off of dust grains, since at the observed distance from the central stars this dust would be too cold to emit thermally in the near-IR. Alternatively, the emission could arise from a faint emission line within J-band bandpass, a possibility which needs to be eliminated in follow-up observations. We note that the jet-like feature is not detected in our H-Band images, likely a consequence of the lower DR in those images (with non-saturated peaks) and/or the lower efficiency of scattering by dust at longer wavelengths.

Assuming scattering by dust, an intriguing interpretation is that this scattering takes place off the inner walls of an evacuated cavity carved by the well-known large-scale outflow. A bipolar outflow was discovered by Poetzel, Mundt, & Ray (1989), traced by several Herbig-Haro objects (blue and red-shifted sides) and a jet (blueshifted side, also SW direction). The total extent of the outflow was 3.6 pc, oriented at $\text{PA}=60^\circ$.

Garcia, Thiébaud, & Bacon (1999) reported an optical jet in [OI] extending approximately $1''$ from Z CMA at PA 240° . The radio counterpart of the outflow was also detected in CO lines (Evans et al. 1994) and in the thermal jet (Velázquez & Rodríguez 2001), both oriented coincident with the optical jet. In the latter case, the high angular resolution of the VLA observations allowed for the first time to clearly identify the origin of the outflow with the SE (FU Ori) binary component. Understanding the shape of the jet-blown cavity and the amount of swept-up dust could constrain the momentum profile of the bipolar winds, testing current theories for such winds and the generation of jets (e.g., Shang, Shu, & Glassgold 1998; Matzner & McKee 1999).

Figure 3 also indicates the direction of the previously known optical jet and bipolar outflow at PA= 240° . If the near-infrared feature arises from light scattering off dust swept-up into a thin shell surrounding a jet-blown cavity, we would expect features on either side of the jet direction (as is also indicated in Figure 3) and both should be (more-or-less) static. However, we do not see any evidence for symmetrical emission on the other side of the optical jet, casting doubt on this hypothesis. On the other hand, the high level of spurious emission may be masking this feature, and even higher dynamic-range observations are needed before this interpretation can be ruled out.

Alternatively, the emission may be directly associated with a different or new jet, given its morphology and association with known accretion objects. If the feature is moving with typical jet velocities (e.g., 500 km/s, Poetzel et al. 1989), then proper motions of the jet feature of up to 100 AU per year (~ 90 mas per year) are expected and should be readily detectable within a short time-span, in contrast to the previous hypothesis.

Unfortunately, due to the PSF artifacts in these first images, the new feature cannot be followed close enough to the central binary to establish whether or not it is associated with one of the components, and higher signal-to-noise at close separations plus optimum placement of the feature with respect to the PSF artifacts may be able resolve this issue.

5. Conclusions

We have detected a new jet-like feature in the close environment of the young stellar binary Z CMA. The feature extends about 1035 AU from the central binary, in the S-SW direction, and has a width of about 115 AU. A symmetric feature to the other side of the known optical jet and bipolar outflow is expected but not detected, and therefore further targeted observations are required to establish whether this new feature is indeed associated with the bipolar outflow (e.g. scattering off dust in its inner walls) or constitutes an independent jet. Our high resolution observations have also revealed for the first time orbital motion in the ZCMA system, as well as further established the high degree of flux variability of its individual components.

R.M.G acknowledges that this work was performed while he was a Michelson Postdoctoral Fellow, funded by the Jet Propulsion Laboratory, which is managed for NASA by the California Institute of Technology. J.D.M. acknowledges support from a Center for Astrophysics Fellowship at the Harvard-Smithsonian Center for Astrophysics. The data presented here were obtained at the W. M. Keck Observatory, which is operated as a scientific partnership among the California Institute of Technology, the University of California, and the National Aeronautics and Space Administration. The observatory was made possible by the generous financial support of the W. M. Keck Foundation. This publication makes use of data products from the Two Micron All Sky Survey, which is a joint project of the University of Massachusetts and the Infrared

Processing and Analysis Center/California Institute of Technology, funded by the National Aeronautics and Space Administration and the National Science Foundation.

REFERENCES

- Akeson, R. L., Ciardi, D. R., van Belle, G. T., Creech-Eakman, M. J., & Lada, E. A. 2000, *ApJ*, 543, 313.
- Barth, W., Weigelt, G., & Zinnecker, H. 1994, *A&A*, 291, 500.
- Danchi, W. C., Tuthill, P. G., & Monnier, J. D. 2001, *ApJ*, 562, 440.
- Evans, N. J., Balkum, S., Levreault, R. M., Hartmann, L., & Kenyon, S. 1994, *ApJ*, 424, 793.
- Garcia, P. J. V., Thiébaud, E., & Bacon, R. 1999, *A&A*, 346, 892.
- Haas, M., Christou, J. C., Zinnecker, H., Ridgway, S. T., & Leinert, C. 1993, *A&A*, 269, 282.
- Hartmann, L. et al. 1989, *ApJ*, 338, 1001
- Heintz, W. D. 1967, *Astronomische Nachrichten*, 289, 269
- Herbig, G. H. 1960, *ApJS*, 4, 337.
- Herbst, W., Racine, R., & Warner, J. W. 1978, *ApJ*, 223, 471.
- Hessman, F. V., Eisloffel, J., Mundt, R., Hartmann, L. W., Herbst, W., & Krautter, J. 1991, *ApJ*, 370, 384
- Koresko, C. D., Beckwith, S. V. W., Ghez, A. M., Matthews, K., & Neugebauer, G. 1991, *AJ*, 102, 2073.
- Malbet, F., Rigaut, F., Bertout, C., & Lena, P. 1993, *A&A*, 271, L9.
- Malbet, F. et al. 1998, *ApJ*, 507, L149.
- Mason, B. D., McAlister, H. A., Hartkopf, W. I., & Shara, M. M. 1995, *AJ*, 109, 332
- Matzner, C. D. & McKee, C. F. 1999, *ApJ*, 526, L109.
- Millan-Gabet, R., Schloerb, F. P., & Traub, W. A. 2001, *ApJ*, 546, 358.
- McLean, I. S. et al. 2000, *Proc. SPIE*, 4008, 1048
- Nakajima, T. & Golimowski, D. A. 1995, *AJ*, 109, 1181.
- Poetzel, R., Mundt, R., & Ray, T. P. 1989, *A&A*, 224, L13.
- Shang, H., Shu, F. H., & Glassgold, A. E. 1998, *ApJ*, 493, L91.
- Thiebaud, E., Bouvier, J., Blazit, A., Bonneau, D., Foy, F.-C., & Foy, R. 1995, *A&A*, 303, 795.
- Tuthill, P. G., Monnier, J. D., & Danchi, W. C. 2001, *Nature*, 409, 1012.
- Velázquez, P. F. & Rodríguez, L. F. 2001, *Revista Mexicana de Astronomia y Astrofisica*, 37, 261.
- Wizinowich, P. et al. 2000, *PASP*, 112, 315

Fig. 1.— Chronology of Z CMa binary separation measurements. We clearly detect a position angle increase of $8.8 \pm 1.5^\circ$ over 11.2 years.

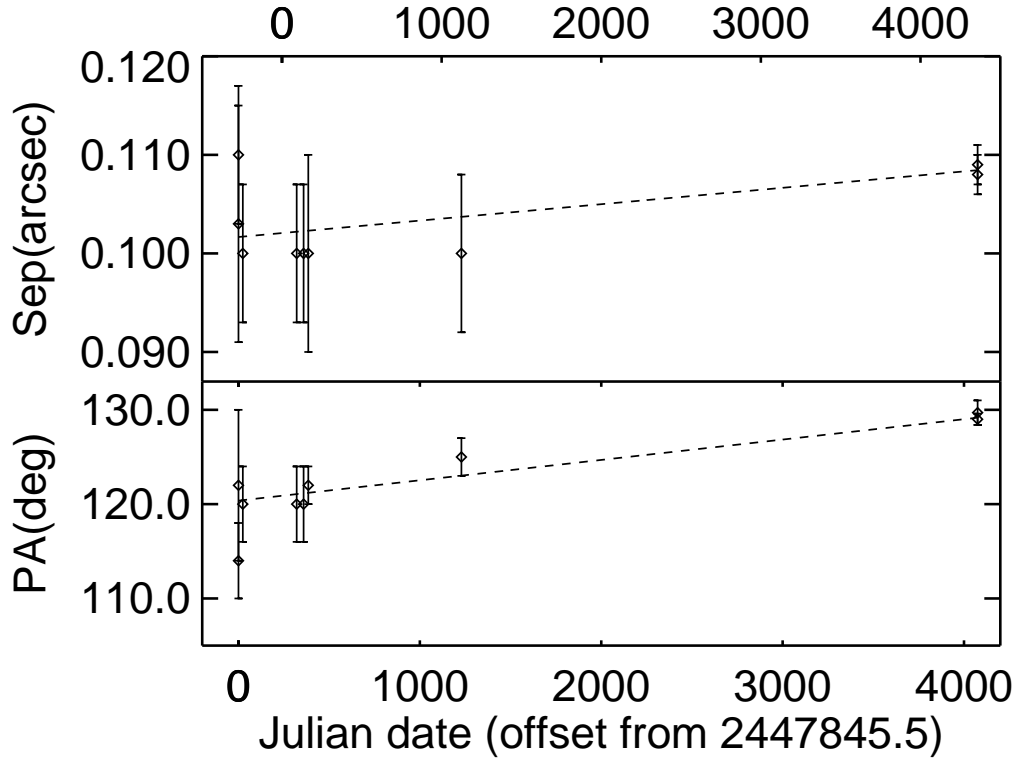


Fig. 2.— High dynamic range images of Z CMa at J-band. Panels (a) & (b) show the mosaiced frames where the new jet is clearly visible amid the PSF artifacts, which repeat in the calibrator observation. The most prominent PSF artifacts are diffraction spikes and internal camera reflections, repeated four times in these images as a result of the mosaicing procedure. We have chosen to display our images in a way that emphasizes the intrinsic detector and optical artifacts, so that the fidelity of the plume structure can be accurately judged.

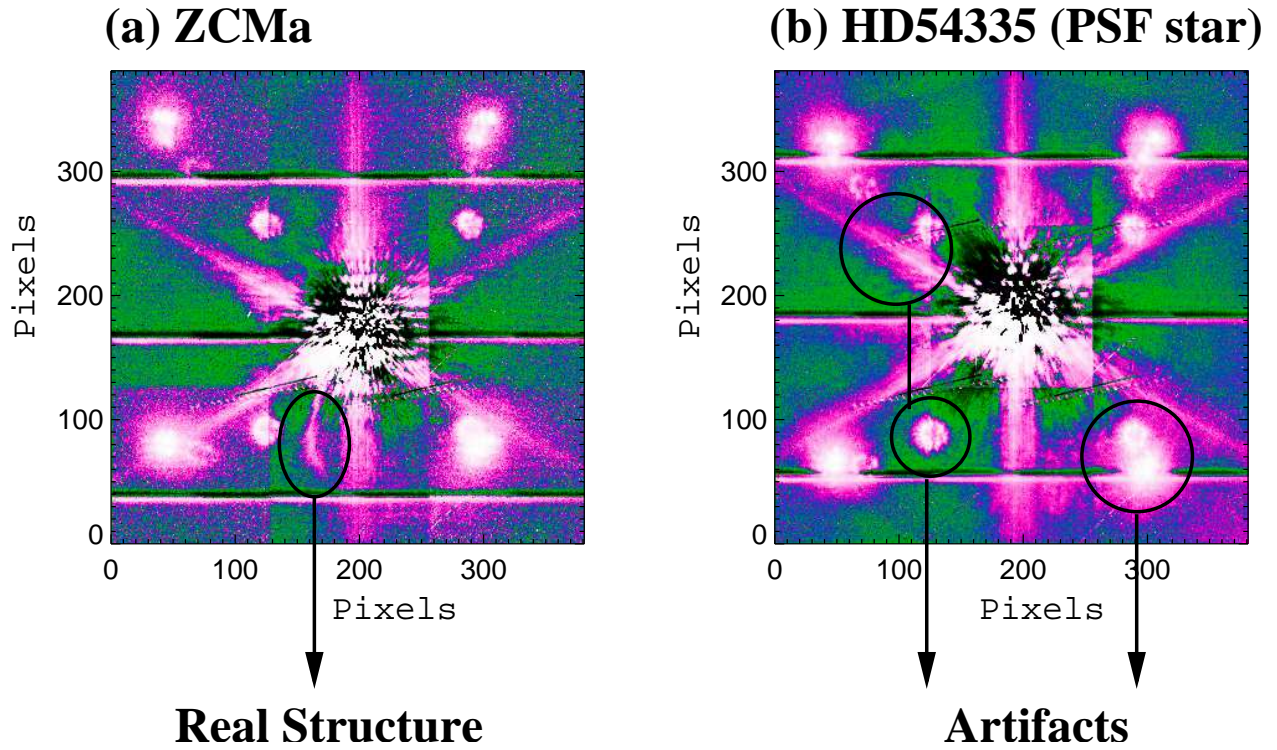


Fig. 3.— High dynamic range images of Z CMA at J-band, centered on the the region near the new jet-like feature. The binary components have been subtracted out of this image, and the color table has been stretched to show the low surface brightness features of the images. This figure also indicates the direction of the known optical jet and bipolar outflow. If the jet-like feature is marking one wall of the jet-blown cavity, we expect to find emission of the cavity wall on the other side of the jet at the location indicated (see discussion in §4).

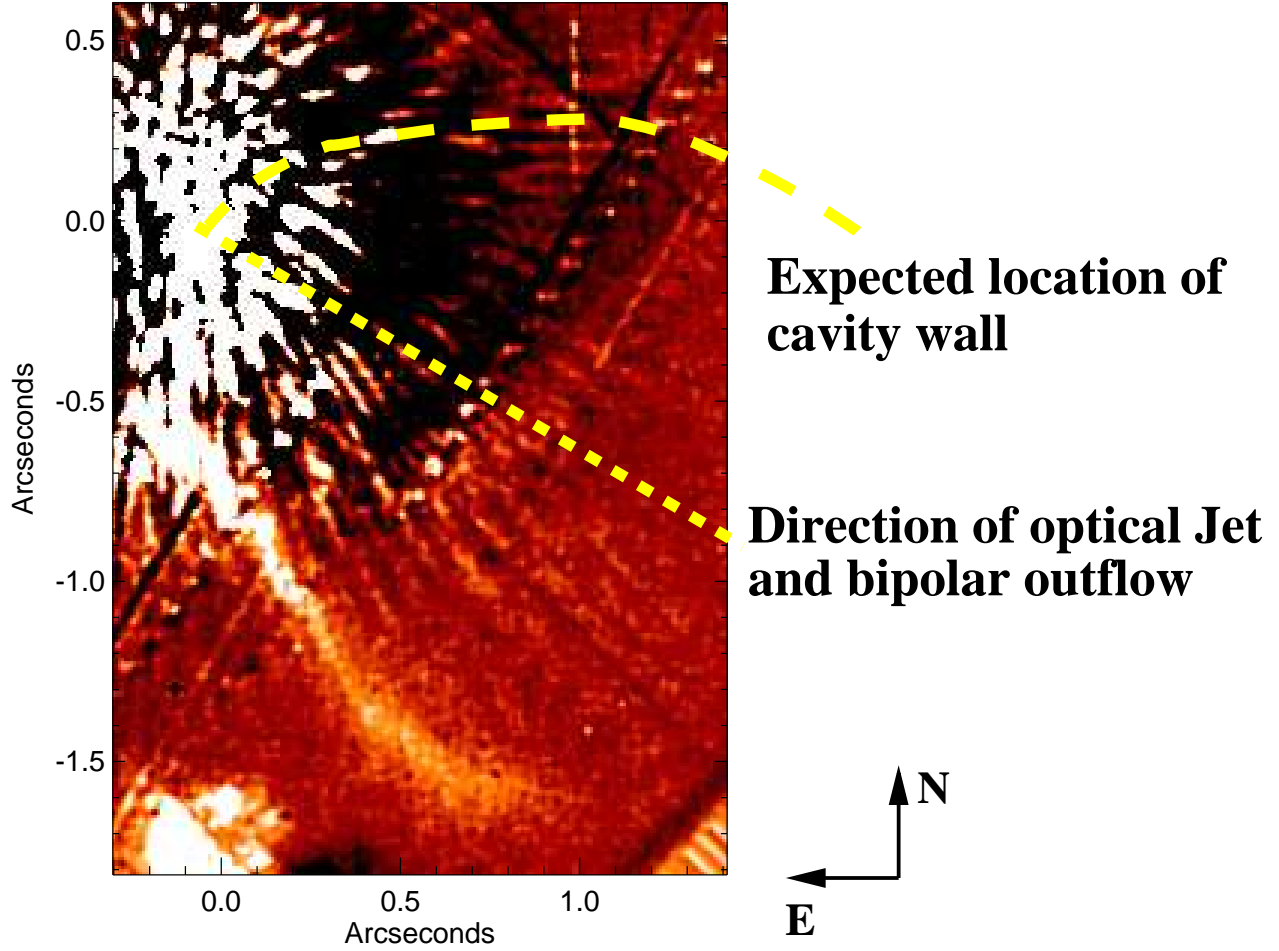


Table 1. Measurements of binary parameters and approximate photometry

Filter	N	Flux Ratio (NW/SE)	Separation (")	PA (°)	Total Flux (Jy)	Flux SE (Jy)	Flux NW (Jy)
J(N3)	4	0.50 ± 0.05	0.109 ± 0.002	129.0 ± 0.6	2.7 ± 0.6	1.8 ± 0.4	0.9 ± 0.2
H(N5)	3	1.18 ± 0.06	0.108 ± 0.002	129.7 ± 1.3	7.9 ± 1.7	3.6 ± 0.8	4.3 ± 0.9